

Resonant Raman scattering and dynamics of the $F_A(\text{Li}^+)$ modes in KCl

M. Leblans, W. Joosen, E. Goovaerts, and D. Schoemaker

*Department of Physics, University of Antwerp (Universitaire Instelling Antwerpen),
Universiteitsplein 1, B-2610 Wilrijk (Antwerpen), Belgium*

(Received 11 August 1986)

By means of the behavior-type method, the polarized resonant Raman intensities of the three $F_A(\text{Li}^+)$ modes in KCl are analyzed, taking into account the optically induced reorientation of the defect. The $F_A(^7\text{Li}^+)$ center is known to possess two high-frequency Raman-active vibrations, at 216 and at 266 cm^{-1} , which exhibit a regular Li^+ isotope shift and a low-frequency resonance at 47 cm^{-1} , which shows a small and anomalous isotope effect. The investigation of their polarized Raman data necessitated an extension of the behavior-type method to the case of resonant scattering. In spite of reorientation effects the Raman scattering excited at the wavelengths of the F_{A1} or F_{A2} band is found to be dominated by the resonant contribution of the defects which can still absorb the incident light. From the analysis of the polarized Raman intensities of the 216- cm^{-1} mode the defect is shown to have only a mirror-plane symmetry, which independently demonstrates the off-axis position of the Li^+ ion in $F_A(\text{Li}^+)$. This deviation from $C_{4v}[001]$ symmetry is not observed in the data for the 47- and the 266- cm^{-1} modes, but within the C_{1h} symmetry group all the modes belong to the representation A' , i.e., they are even under reflection. The polarized Raman study, together with the isotope shifts of the Raman modes and considerations of the normal modes of the defect, permits a more detailed description of the dynamics of the $F_A(\text{Li}^+)$ center: The 266- and the 216- cm^{-1} vibrations strongly involve the Li^+ -ion motion within the mirror plane, essentially parallel and perpendicular to the defect axis, respectively. The low-frequency mode at 47 cm^{-1} is an activated band mode in which the Li^+ ion hardly participates, similar to the 43- cm^{-1} mode of the naked Li^+ impurity.

I. INTRODUCTION

The $F_A(\text{Li}^+)$ center in KCl was identified by optical absorption^{1,2} and electron-nuclear double resonance.³ It consists of an F center perturbed by a Li^+ impurity which replaces a nearest-neighbor (NN) K^+ ion. The optical absorption and luminescence spectra were extensively investigated.⁴ The optical F -band transition from the s -like ground level to the p -like excited level is split up into a σ -polarized F_{A1} band at 630 nm, and a π -polarized F_{A2} band at 550 nm. Excitation of these optical transitions induces reorientation of the centers, which still takes place efficiently down to 2 K.⁴

After the pioneering Raman studies of Worlock and Porto⁵ on the F center, the $F_A(\text{Li}^+)$ defect was the second color center to be investigated with this technique.⁶ Besides an F -center-like first-order defect-induced phonon spectrum consisting of two broad bands in the region between 50 and 213 cm^{-1} , the $F_A(\text{Li}^+)$ center possesses three Raman-active vibrational modes at 47, 216, and 266 cm^{-1} (for the ^7Li isotope). Because of the failure to explain the polarized Raman intensities, together with the large positive isotope shifts of the high-frequency modes under ^7Li to ^6Li substitution, on the basis of scattering from A_1 or E localized modes in a C_{4v} defect symmetry, it was proposed that the Li^+ ion in $F_A(\text{Li}^+)$ is not located on the K^+ site, but is off axis in one of four equivalent potential minima. The off-axis position of the Li^+ ion was confirmed by electro-optical experiments⁷ and determined to lie in a $\{110\}$ plane with respect to the main

$\langle 100 \rangle$ defect axis. Recently, the tilting of the p -type orbitals of the $F_A(\text{Li}^+)$ center as a result of the off-axis Li^+ position was quantitatively determined by refined absorption and emission measurements.⁸ Further Raman experiments on the $F_A(\text{Li}^+)$ center have demonstrated the dependence of the spectral distribution and the polarized Raman intensities on the excitation wavelength.^{9,10} It was also found that the high-frequency modes possess a regular isotope shift under ^7Li to ^6Li substitution, while the low-frequency mode shows a small and negative isotope effect.

The off-axis Li^+ position in an $F_A(\text{Li}^+)$ center is not totally unexpected, considering that the naked Li^+ impurity in KCl is a well-known $\langle 111 \rangle$ off-center defect with tunneling behavior.¹¹ In the $F_A(\text{Li}^+)$ center the Li^+ ion is probably also tunneling between the four potential minima (Refs. 6 and 7 and Sec. V in Ref. 12). As was observed in both Raman¹⁰ and infrared¹³ (ir) measurements, the naked Li^+ impurity possesses a low-frequency mode with a similar anomalous isotope effect ($\sim 1.1 \text{ cm}^{-1}$) as the 47 cm^{-1} mode of $F_A(\text{Li}^+)$. Both from a theoretical study¹⁴ and from the analysis of the polarized Raman spectra¹⁵ this mode of the naked Li^+ was demonstrated to be an activated band mode in which essentially no Li^+ motion is involved. The calculation by Sangster and Stoneham¹⁴ yields, for the Li^+ impurity, two high-frequency localized modes which, however, were observed neither in infrared absorption, nor in Raman scattering.

In this paper polarized Raman spectra of $F_A(\text{Li}^+)$ in KCl under F_{A1} and F_{A2} resonant excitation, and under

nonresonant excitation at 676.4 nm are presented and analyzed by means of the behavior-type (BT) method.^{16,17} Special care was taken to secure accurate polarization and crystal axes orientation, since the polarized Raman intensities are extremely sensitive to misalignment, mainly because of the reorientation properties of $F_A(\text{Li}^+)$. This has resulted in discrepancies between earlier reported measurements.^{6,9,10} Other effects of the optical reorientation of the defects are accounted for in the analysis. The BT method was applied before to a series of defects in alkali halides (Refs. 15 and 18–20), but in the present case a generalization to resonant Raman scattering (RRS) was necessary. The question formulated by Fritz,⁶ whether or not the resonant contribution to the Raman spectrum is dominant under F_A excitation, will be answered. It is also demonstrated that the polarization properties of the F_{A1} and F_{A2} bands drastically influence the polarized Raman intensities through selective resonant enhancement,¹⁸ which obscures the nature of the vibrational modes. Combination of these results and comparison with earlier investigations on $F_A(\text{Li}^+)$ and Li^+ in KCl leads, for the first time, to a complete and consistent interpretation of the nature of the three Raman modes of $F_A(\text{Li}^+)$.

II. EXPERIMENTAL PROCEDURES

Details about the Raman equipment are given in Ref. 19. The resolution of the spectrometer was set at 2 cm^{-1} . The temperature during the Raman measurements was 10 K. The exciting wavelength has been tuned from 676.4 to 457.9 nm, i.e., through the F_{A1} band, the F_{A2} band, and the higher optical absorption bands of $F_A(\text{Li}^+)$. A Rhodamine-6G dye laser, pumped by an Ar^+ -ion laser was employed, and furthermore, the He-Ne laser line at 632.8 nm and the Kr^+ -ion laser lines at 676.4 and 647.1 nm. The intensities varied between 3 and 50 mW for the resonant spectra and was 100 mW for the 676.4-nm laser line, which is not at resonance with the F_{A1} or F_{A2} bands of $F_A(\text{Li}^+)$.

The KCl samples, grown from melts containing 2×10^{-2} wt. % of LiCl were x irradiated for 30 min at room temperature to produce F centers. Next, the F centers were converted to F_A centers at 250 K by light from a Hg lamp filtered by a broadband interference filter (centered at 250 nm with 100 nm half-width) for 30 min and kept in the dark for 15 min at the conversion temperature. This way, the conversion is—on purpose—not very efficient and complete, but treatment of the sample with F light resulted in the presence of other unidentified Li^+ -related defects, whose Raman spectra partially overlap the modes of $F_A(\text{Li}^+)$. Due to the presence of the F centers besides the $F_A(\text{Li}^+)$ centers, the $F_A(\text{Li}^+)$ spectrum under F_{A2} excitation may be superimposed on an F -center contribution.

In contrast to additively colored crystals,⁴ the $F_A(\text{Li}^+)$ centers in x -irradiated crystals undergo thermal dissociation after optical excitation. This is taken into account by measuring the different polarized Raman spectra a second time, but in reversed sequence. Afterwards, the corresponding spectra were added and the resulting polarized data are presented in the figures.

III. RAMAN SCATTERING AND OPTICAL ABSORPTION PROPERTIES OF $F_A(\text{Li}^+)$ IN KCl

A. Dependence of the resonant Raman intensities on the exciting wavelength

Three illustrative sets of polarized Raman spectra of $F_A(\text{Li}^+)$, obtained under 600, 632.8, and 676.4 nm excitation are presented in Fig. 1. The measured intensities of a given vibrational mode, $I_{a,b}$ (a and b indicate the polarization directions of incident and scattered light), are related to the so-called intensity parameters (IP's) q_i , r_i , and s_i (Refs. 16 and 17), which are of fundamental importance in the BT analysis. These intensities are given for Fig. 1(a) by

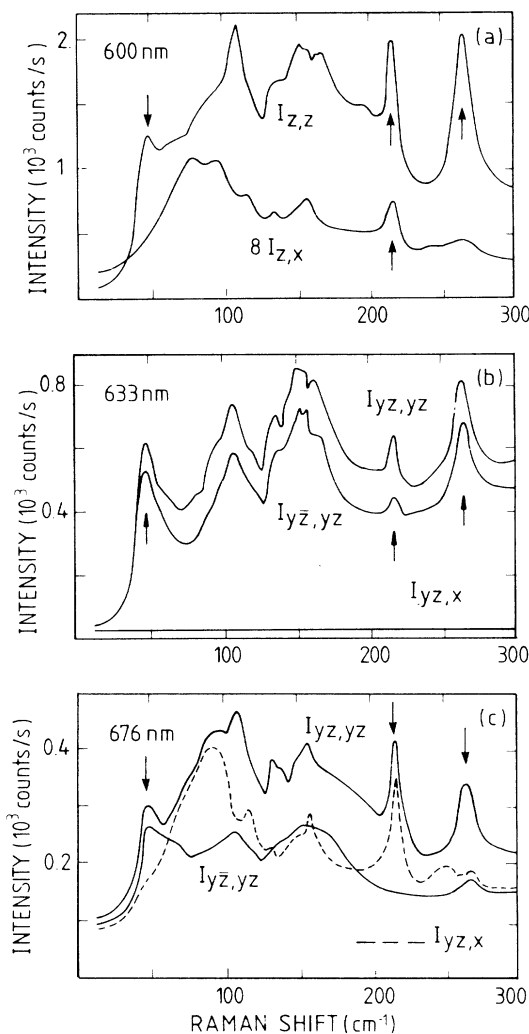


FIG. 1. The polarized Raman spectra of $F_A(\text{Li}^+)$ in KCl at 10 K under (a) 600 nm resonant excitation between the F_{A1} and F_{A2} band (40 mW); (b) 632.8 nm resonant excitation in the F_{A1} band (3 mW); (c) 676.4 nm nonresonant excitation (100 mW). The spectra (a) are obtained in the scattering geometry shown in Fig. 2(a); spectra (b) and (c) in the geometry of Fig. 2(b).

$$I_{z,z} = q_3, \quad I_{z,x} = s_2, \quad (1)$$

and are measured in the scattering geometry illustrated in Fig. 2(a). For the spectra of Figs. 1(b) and 1(c) the intensities are measured in the geometry of Fig. 2(b) and are given by

$$I_{yz,yz} = \frac{1}{2}(q_2 + r_1) + s_1, \quad (2a)$$

$$I_{\bar{y}\bar{z},yz} = \frac{1}{2}(q_2 - r_1), \quad (2b)$$

$$I_{\bar{y}\bar{z},x} = I_{yz,x} = s_2. \quad (2c)$$

In the latter equations it is taken into account that the representative symmetry F_1 of the orientating operator, which represents the laser-induced distribution of the defects among their possible orientations in the crystal is equal to $D_4[100]$ (see also Sec. IV A). The axes are labeled such that the fourfold symmetry axis of F_1 lies along $[100]$, corresponding to the case considered in Ref. 16. The scattering geometry is not considered in Ref. 16, but the above equations can be easily derived from the general relation between the scattered intensity $I_{a,b}$ and the intensity parameters.

From the polarized spectra the values of q_i , r_i , and s_i are derived for the three modes of $F_A(\text{Li}^+)$ and for the different excitation wavelengths. The q_i parameters are found to be nonzero for each of the three modes, while in most of the cases the ratio s_i/q_i is equal to zero within experimental error. Only for the 216-cm^{-1} mode and the phonon continuum nonzero s_i/q_i values are found for F_{A2} and nonresonant excitation.

The Raman scattering intensities of the 266- and 47-cm^{-1} modes are relatively more intense than that of the 216-cm^{-1} mode under F_{A1} excitation. Under F_{A2} excitation the 216- and 266-cm^{-1} modes are equally intense, but at shorter excitation wavelengths the latter weakens (e.g., at 514.5 nm , see Ref. 9) and finally it is not observed anymore. The 47-cm^{-1} mode is not observed under F_{A2} excitation.

A more striking illustration of the dependence of the spectral distribution on the exciting frequency is that under F_{A1} and F_{A2} excitation the spectra corresponding to the s_2 parameters [$I_{x,z}$ in Fig. 1(a) and $I_{yz,x}$ in Fig. 1(b)] are very small with respect to the intensities of other polarization geometries, but that for nonresonant excitation [Fig. 1(c)] both the phonon continuum and the 216-

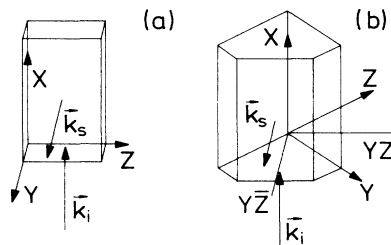


FIG. 2. The scattering geometries employed for the polarized Raman measurements. \mathbf{k}_i and \mathbf{k}_s are the wave vectors of the incident and the observed scattered beam, respectively. x , y , and z are the crystal axes. The BT analysis of the Raman spectrum of $F_A(\text{Li}^+)$ is based upon measurements in the geometry (b).

cm^{-1} mode have comparable intensities in the different polarization geometries.

B. Optical absorption and reorientation behavior

For a given frequency and polarization of the incident light beam a reorientation of the $F_A(\text{Li}^+)$ centers occurs, resulting in a particular stationary distribution of the defects among the six possible configurations of the vacancy with respect to the Li^+ impurity⁴ (see Fig. 3), such that the orientation most strongly absorbing the incident light, will possess the lowest population number. Only three independent population numbers have to be considered, since Raman measurements cannot discern between configurations related by inversion. We have verified by means of optical-absorption measurements that the stationary distribution⁸ is reached within a second under conditions of laser illumination as used in the Raman experiments (Sec. III D of Ref. 18).

The p_z (p_x and p_y) orbital of the excited electronic state is mixed with a small amount of p_x and p_y (p_z),⁸ which means that the F_{A1} (F_{A2}) transition is not 100% σ - (π -) polarized. The orbitals are tilted away from the crystal axes as a result of the off-axis position of the Li^+ ion away from the substitutional K^+ site. The magnitude of the tilting influences the absorption of the incident light, and hence the reorientation rates and the stationary distribution of the center. Taking advantage of this effect, Bal-dacchini *et al.*⁸ determined a value of 8° for the tilting angle.

The resonant enhancement of the scattering and the dependence of the population numbers on the polarization of the laser light, imply an extreme sensitivity of the resonant Raman spectra to the orientation of the sample. This situation has given rise to some discrepancies between different sets of resonant Raman data published up till now.^{6,9,10} It necessitated additional polarized Raman measurements to achieve a suitable input for the BT analysis. The correct orientation of the crystal can be

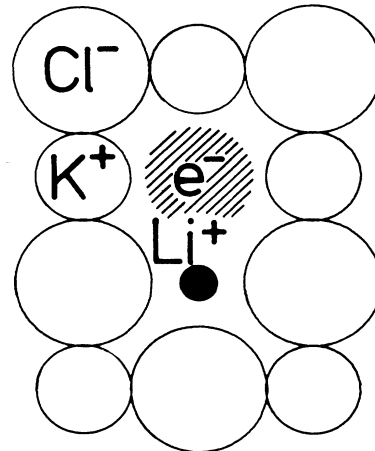


FIG. 3. Schematic picture of the $F_A(\text{Li}^+)$ on-center model. Upon optical excitation in the F_{A1} or F_{A2} absorption band the direction of the defect axis can change.

checked by verifying the specific relations that exist between the polarized Raman intensities, which are valid regardless of the defect symmetry.¹⁶

IV. BEHAVIOR-TYPE ANALYSIS OF THE POLARIZED RAMAN DATA

A. Resonant Raman scattering and reorientational effects

The behavior-type (BT) method was developed to analyze polarized Raman data of an observed dynamical mode of a defect in a cubic crystal.^{16,17} The method permits one to determine within clearly spelled-out limits the defect symmetry and the irreducible representation of the Raman mode.

Two important problems arise when the BT method is applied to the analysis of the Raman data of $F_A(\text{Li}^+)$ in KCl.

(1) The resonant character of the Raman scattering implies the eventual occurrence of asymmetric tensors. However, the BT method was developed to interpret non-resonant Raman spectra and deals exclusively with symmetric Raman tensors. The arguments given in Ref. 18, applying this method also in the case of resonant scattering, are not valid here. Therefore, an extension of the method to resonant Raman scattering has been worked out and is briefly discussed in the Appendix. For the purpose of presentation, the analysis below employs the BT method for nonresonant Raman scattering. We verified that as far as the modes of $F_A(\text{Li}^+)$ are concerned, the BT method for resonant Raman scattering yields the same final conclusion for the actual defect symmetry and the representations of the modes.

(2) The polarized incident laser light itself reorients the $F_A(\text{Li}^+)$ centers and as such, it acts as an orientating operator \hat{F} , crucially depending on the polarization direction and the wavelength, as discussed in the preceding section. A set of IP's, which leads to a meaningful interpretation by means of the BT method, must be obtained for one particular \hat{F} , with a corresponding set of population numbers of the center in the various orientations. In practice, this means that during the Raman experiment, a variation of the polarization direction or the wavelength of the laser light should not change the population numbers. On the other hand, the Raman intensities have to be measured for several incoming and outgoing polarizations of the light, in order to obtain a conclusive set of polarized Raman data. A suitable geometry for this purpose is shown in Fig. 2(b). Taking into account the reorientation properties of $F_A(\text{Li}^+)$, this geometry yields the same representative symmetry of the orientating operator ($F_1 = D_4[100]$) and the same population numbers for a $[011]$ and a $[01\bar{1}]$ polarization of the incident beam. Implicitly we have assumed that, if the Li^+ ion occupies an off-axis position, the four equivalent off-axis positions corresponding to a given $\langle 100 \rangle$ orientation, possess the same population number as a result of fast hopping or tunneling between these positions.

B. Behavior-type analysis and determination of the actual symmetry and representations of the modes

The BT analysis is based upon measurements in the scattering geometry shown in Fig. 2(b) and discussed in Secs. III A and IV A. The BT which can occur together with $F_1 = D_4[100]$ are listed in Tables VII and VIII of Ref. 16. The modes of $F_A(\text{Li}^+)$ must necessarily possess one of these BT.

1. Polarized Raman intensities of the 47- and 266-cm⁻¹ modes pointing to a C_{4v} symmetry

The polarized Raman intensities of the low-frequency mode at 47 cm⁻¹ and the high-frequency mode at 266 cm⁻¹ possess the same observed BT. The s_2 IP is equal to zero for all of the employed exciting wavelengths. This means that s_1 and s_3 are also equal to zero, which is immediately verified in Table VII of Ref. 16. In this case, one can calculate r_1 from the experimental intensities and Eqs. (2a) and (2b). Consequently, the BT relations are

$$q_2 \neq 0, \quad 0 \leq r_1 < q_2, \quad s_1 = s_2 = s_3 = 0. \quad (3)$$

The above relations define BT 29, which corresponds to the following representative modes (Tables VII and VIII in Ref. 16):

$$D_2[100]:A, \quad C_4[001]:A, \quad D_4[001]:A_1. \quad (4)$$

The representative modes (4) represent 11 actual modes (Table VI, Ref. 16), but one cannot discriminate between the latter by means of the BT method. We take into account now, that $F_A(\text{Li}^+)$ consists of a Li^+ impurity and an adjacent F center. The Li^+ ion can be positioned on or away from a $\langle 100 \rangle$ crystal axis. In the latter case, the symmetry group of the defect does not belong to one of the representative symmetries in (4), whereas in the former the symmetry group of the defect is C_{4v} , belonging to the representative symmetry D_4 . This leaves one with $C_{4v}:A_1$ modes for the modes at 47 and 266 cm⁻¹.

2. The 216-cm⁻¹ mode and the off-center position of Li^+

Under F_{A1} excitation, the same BT is observed for the 216-cm⁻¹ mode as for the two other modes. However, under F_{A2} excitation the mode at 216 cm⁻¹ possesses different polarization properties, which is even more obvious under 676.4 nm nonresonant excitation (Fig. 1).

The following BT relations are observed for the 216-cm⁻¹ mode:

under F_{A1} excitation:

$$q_1 \neq 0, \quad 0 < r_1/q_2 < 1, \quad s_2 = 0, \quad (5a)$$

under F_{A2} excitation:

$$q_2 \neq 0, \quad s_2 \neq 0. \quad (5b)$$

From Eqs. (2) (Sec. III A) one can see that r_1/q_2 cannot be determined from the measurements when $s_1 \neq 0$. The observed BT must be consistent with the data obtained both under F_{A1} and under F_{A2} excitation. At this point it is useful to remark that several BT's possess the relation $r_2/q_1 = -\frac{1}{2}$. This relation cannot be verified, since the

reorientation properties of $F_A(\text{Li}^+)$ allow one to measure r_1 and q_2 only. However, the relation $r_1 \geq 0$ (under F_{A1} excitation) is sufficient to eliminate these BT's. For this reason, e.g., the modes belonging to the B representation of the $C_2[110]$ and the B_1 of the $D_2[110]$ representative symmetries are excluded. The BT consistent with Eqs. (5) is BT 58 and the corresponding representative modes are

$$C_1:A, C_2[010]:A, C_2[110]:A, D_2[110]:A. \quad (6)$$

A similar argument as in Sec. IV B 1 yields the $C_{1h}(010):A'$ or the $C_{1h}(110):A'$ modes out of the 12 actual modes included in these representative modes (6). Hence, an off-axis position of the Li^+ ion is compatible with the polarized Raman data of the 216-cm^{-1} mode. The most general mode $C_1:A$ is not considered.

The results of the BT analysis are remarkable in the sense that the three modes of $F_A(\text{Li}^+)$ possess observed BT's belonging to two different symmetries, although they belong to the same defect. In the next section it will be explained that this is not contradictory.

V. INTERPRETATION OF THE BEHAVIOR-TYPE ANALYSIS AND THE DYNAMICS OF $F_A(\text{Li}^+)$

A. Off-center position of the Li^+ ion in $F_A(\text{Li}^+)$ in KCl

Incidentally, the observed BT exhibits a higher symmetry than the actual mode symmetry (Sec. II E in Ref. 16). From Table X of Ref. 16 one derives all possible *actual* BT's corresponding to the *observed* one and occurring for the same symmetry of the orientating operator. The more general actual BT corresponding to BT 29, observed for the 47- and 266-cm^{-1} modes, is BT 58, observed for the 216-cm^{-1} mode. Hence, it is concluded that the three modes in the Raman spectrum of $F_A(\text{Li}^+)$ in KCl can be considered $C_{1h}:A'$ modes.

Note that the Raman data *alone* are sufficient to establish the off-axis position of the Li^+ ion in $F_A(\text{Li}^+)$. The vibrational motion of the ions participating in the A' Raman modes, are even with respect to the mirror plane. In particular, if the Li^+ ion participates in the motion, it necessarily moves within the mirror plane.

From our measurements and the BT method it is not possible to prove whether the plane of symmetry is either a $\{110\}$ or a $\{010\}$ plane. By means of electro-optical modulation spectroscopy, Rosenberger and Lüty⁷ concluded that the four potential minima lie in $\{110\}$ planes through the defect axis.

B. Dynamics of the modes of $F_A(\text{Li}^+)$ in KCl

1. Symmetry of the Li^+ coordinates

If we first consider the Li^+ coordinates in a C_{4v} model, i.e., a model in which Li^+ is lying on a $\langle 100 \rangle$ crystal axis, the coordinate along the fourfold axis belongs to A_1 , while the two coordinates perpendicular to it belong to the E representation. When the ion goes off-axis in a $\{110\}$ plane the A_1 coordinate, as well as the E coordinate which describes the motion within this mirror plane, turn into $C_{1h}:A'$ modes (see Fig. 4). The other E coordinate

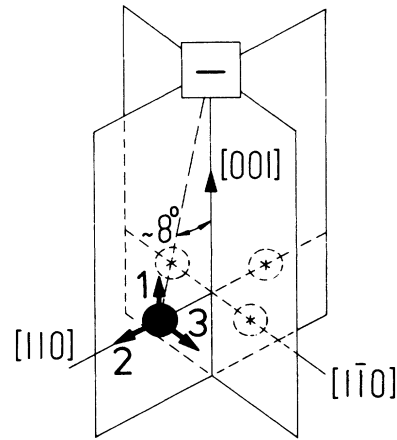


FIG. 4. Schematic model of $F_A(\text{Li}^+)$ in KCl, showing the Li^+ ion next to the F center, and its four equivalent off-axis positions lying along the $\langle 110 \rangle$ directions perpendicular to the center axis. The Li^+ vibrational coordinates 1 and 2 within the $(\bar{1}\bar{1}0)$ mirror plane are associated with the 266- and the 216-cm^{-1} modes, respectively. The Li^+ coordinate 3 perpendicular to the mirror plane is not observed in the Raman spectrum.

describes the Li^+ mode perpendicular to the mirror plane and belongs to $C_{1h}:A''$. A vibrational mode belonging to $C_{1h}:A''$ which would possess BT 45a, did not appear in the $F_A(\text{Li}^+)$ spectra. This is not fully understood, but it could be related to the tunneling motion of the Li^+ ion which takes place perpendicular to the mirror plane, or result from strong coupling of this mode with lattice phonons such that it becomes a very broad resonance.

2. $F_A(\text{Li}^+)$ modes involving Li^+ motion

As witnessed by the significant isotope shifts,^{6,10} the 216-cm^{-1} and 266-cm^{-1} modes strongly involve Li^+ vibrations. For the 266-cm^{-1} mode the shift is very close to that expected from the isotope mass ratio for a pure Li^+ vibration, while for the 216-cm^{-1} mode a smaller shift is found, indicating admixture of vibrational coordinates of the surrounding ions. The 216-cm^{-1} mode lies close to the edge of the optical-phonon frequencies ($\omega_{\max} = 213 \pm 3 \text{ cm}^{-1}$) (Ref. 21) which favors coupling to the phonons.

The 266-cm^{-1} mode possesses BT 29 for all of the exciting wavelengths, corresponding to a $C_{4v}:A_1$ mode. This strongly suggests that this mode mainly derives from the Li^+ motion parallel to the main $\langle 100 \rangle$ center axis, corresponding to the Li^+ coordinate (1) in Fig. 4. Therefore and because it is the only mode possessing $s_i/q_i \neq 0$, we identify the 216-cm^{-1} mode with a perpendicular Li^+ vibration, i.e., the $C_{1h}:A'$ mode deriving from $C_{4v}:E$ [coordinate (2) in Fig. 4]. These qualitative features agree quite well with the high-frequency modes of the Li^+ impurity calculated by Sangster and Stoneham¹⁴ which, however, were not observed. In the $F_A(\text{Li}^+)$ Raman spectra they occur, probably as a result of the high polarizability acquired from the adjacent F center.

In fact, it may seem surprising that a mode which is associated with a $C_{4v}:E$ would behave nearly like a $C_{4v}:A_1$ mode in the resonant polarized spectra. This results from

selective resonant enhancement of particular Raman tensor components (see Sec. VD).

3. Character of the low frequency $F_A(\text{Li}^+)$ mode

The 47-cm^{-1} mode of $F_A(\text{Li}^+)$ possesses a small and anomalous Li^+ isotope shift, and therefore it is not expected to involve a significant Li^+ motion. Moreover, the Li^+ coordinates with $C_{1h}:A'$ symmetry are exhausted by the two high-frequency modes. The observed BT points to a $C_{4v}:A_1$ mode, i.e., the off-axis Li^+ position is not reflected in its polarized Raman intensities.

These results are reminiscent of the findings for the low-frequency mode at 43 cm^{-1} of the naked Li^+ impurity in KCl. Also for this $\langle 111 \rangle$ off-center impurity the ir and Raman modes show a small and anomalous isotope shift.^{10,13} Recently we have demonstrated that the Raman mode exhibits $O_h:A_{1g}$ symmetry and have proposed that it essentially consists of a totally symmetric vibration of the surroundings in which the Li^+ ion is hardly involved.¹⁵ Previously, Sangster and Stoneham¹⁴ have drawn a similar conclusion from a computation of the phonon density of states of a finite crystal perturbed by a Li^+ impurity.

The striking analogy between the low-frequency modes of the naked Li^+ impurity and the $F_A(\text{Li}^+)$ center leads us to the following conclusion: The 47-cm^{-1} mode of $F_A(\text{Li}^+)$ is a totally symmetric mode in C_{4v} symmetry, mainly involving the ions surrounding the Li^+ ion. Neither the vibrational coordinate of this mode, nor the Raman tensor are significantly influenced by the Li^+ off-axis position. The small anomalous isotope shift very probably stems from the coupling between the Li^+ tunneling motion and the lattice vibrations.²²

C. Reduced resonant Raman intensity due to optical reorientation

The reorientation properties of $F_A(\text{Li}^+)$ and the resonance condition raise some fundamental questions about the origin of the Raman intensities. The polarized Raman intensities can be expressed as

$$I_{a,b} = kI_0 \sum_n \sum_{i,j,k,l} a_i b_j a_k b_l N^{(n)} T_{ij}^{(n)} T_{kl}^{(n)}.$$

$N^{(n)}$ is the population number and $T_{ij}^{(n)}$ are the Raman tensor elements, both for the n th orientation of the defect. \mathbf{a} and \mathbf{b} are the polarization vectors for the incident and scattered light.

For particular polarizations and wavelengths of the incident laser light (e.g., $I_{y,y}$ under F_{A1} and F_{A2} excitation), the resonance condition enhances only the $T_{ij}^{(n)}$ corresponding to the orientations which absorb the light. However, it also induces optical reorientation which depopulates these orientations, while large population numbers correspond to orientations which do not absorb the incident light and possess $T_{ij}^{(n)}$ which are not resonantly enhanced under the exciting wavelength. Hence, the question arises what terms in the polarized Raman intensity dominantly contribute to these polarized Raman intensities.⁶

We found that in general, the total Raman intensity

must be regarded as a superposition of F_{A1} and F_{A2} contributions, but with dominant F_{A1} (F_{A2}) contribution under F_{A1} (F_{A2}) excitation, as will be shown below. As such, the Raman spectral features of $F_A(\text{Li}^+)$ can be interpreted as if the center were static and are comparable, e.g., with those of the $\text{Tl}^0(1)$ center, which does not optically reorient appreciably during the Raman measurements.¹⁸

Under F_{A2} excitation with polarization parallel to [011], all orientations absorb the incoming light. As a result, neither one of the three orientations is substantially less populated. This means that the F_{A2} contribution to the Raman spectrum exceeds the F_{A1} contribution. In the case of [010] polarization, almost all centers are in an unfavorable orientation to scatter the light resonantly. However, the spectrum exhibits the same characteristics as in the [011] polarization case. Hence, with the incident polarization along [010], the F_{A2} contribution to the spectrum is dominant in spite of the reorientation behavior.

For F_{A1} excitation polarized along [010] and [011] the orientation(s), which resonantly scatter(s) the laser light, are nearly completely depleted. Hence, one may expect a weak contribution from the F_{A1} band. With [112] polarized F_{A1} light,⁶ all orientations of the center absorb the incident beam. Thus we may be sure to observe a Raman spectrum to which mainly F_{A1} contributes. Nevertheless, the relative intensities in this spectrum are the same as in the Raman spectra with [010] and [011] polarized incident laser light.⁶ One concludes that under F_{A1} excitation the F_{A1} contribution to the Raman scattering is dominant, even with [010] and [011] polarized incident light. In contradiction with our results it was concluded in Ref. 6 from the same [112] polarization experiment that F_{A1} scattering plays a minor role, if any, in the Raman spectra under F_{A1} excitation. This interpretation, however, is not consistent with two different types of Raman spectra obtained under F_{A1} and F_{A2} excitation (see Fig. 1).

D. Selective resonant enhancement of the Raman tensor elements

Selection rules for the Raman scattering of a mode and the form of its Raman tensor are determined by the defect symmetry and the representation to which the vibrational mode belongs. Furthermore, in the case of resonant Raman scattering, the symmetry properties of the electronic transitions, which are resonantly excited by the incident light, restrict the tensor elements which can be resonantly enhanced.

The selective resonant enhancement in a C_{4v} symmetry is discussed in Ref. 18. Deviations from these rules, due to the off-axis position of the Li^+ ion are small, since they are closely related to the optical properties of the F_{A1} and the F_{A2} band, which are fairly well described by the C_{4v} symmetry.⁴ One concludes the following.

(i) Only $C_{4v}:A_1$ modes can be resonantly enhanced by the F_{A1} band.

(ii) The F_{A2} band enhances $C_{4v}:A_1, A_2, B_1, B_2$ modes.

(iii) $C_{4v}:E$ modes can be resonantly enhanced neither in the F_{A1} nor in the F_{A2} band.

The selective resonant enhancement is nicely demon-

strated by comparison of the resonantly excited and the off-resonance excited Raman spectra through the s_i/q_i ratio. It explains the zero s_i/q_i ratio under F_{A1} excitation and the extreme small s_i/q_i under F_{A2} excitation over the whole Raman spectrum. This is true in particular for the mode at 216 cm^{-1} , which possesses mainly E character. *This mode can only be resonantly enhanced if its Raman tensor departs from that of an exact $C_{4v}:E$ mode and as a consequence, it is the only mode which reveals the off-axis Li^+ position.* Moreover, in C_{1h} symmetry only the A' mode can be resonantly enhanced in both the F_{A1} and F_{A2} band, and also possess off-diagonal elements which are resonantly enhanced under F_{A2} excitation. The latter results in nonzero values of s_i/q_i . These properties are completely consistent with the behavior of the 216-cm^{-1} mode.

The 266-cm^{-1} mode appears more strongly in the Raman spectrum than the 216-cm^{-1} mode under F_{A1} excitation, while this is not the case under F_{A2} excitation. This means that it possesses a more important T_{33} Raman tensor element. Since a motion of the Li^+ ion parallel to the defect axis can be expected to affect the p_z -like orbital more than the p_x - and p_y -like orbitals, this intuitive argument is also consistent with our interpretation of the dynamics of the modes.

VI. CONCLUSIONS

The first Raman measurements on $F_A(\text{Li}^+)$ in KCl were already demonstrated by Fritz to be *inconsistent* with a C_{4v} on-center impurity model; an off-axis position of the Li^+ ion was proposed and subsequently confirmed by other experimental techniques. We have analyzed the polarized Raman data for several excitation frequencies, by means of the behavior-type method, which we extended for the case of RRS. The analysis provides *direct* evidence for the C_{1h} point group, which is the instantaneous defect symmetry of $F_A(\text{Li}^+)$. The A' character of its three modes has also been established. This Raman result and the isotope shifts of the modes under ^7Li to ^6Li substitution allow a more profound insight in the ionic motions involved in each of the Raman modes. As such this study demonstrates the usefulness of the BT method for a defect system to which a lot of previous Raman work has been devoted.

The most peculiar Raman feature of the $F_A(\text{Li}^+)$ center is its 216-cm^{-1} mode, which reflects the off-axis position of the Li^+ vibration perpendicular to the center axis and can be considered as a perturbed $C_{4v}:E$ mode. However, its polarized Raman intensities hardly look as if they originate from such a mode of which the only nonzero Raman tensor components are off-diagonal. It is precisely the deviation from the exact C_{4v} symmetry, which allows the diagonal components of the Raman tensor to be nonzero, and the latter are resonantly enhanced under F_{A1} and F_{A2} excitation.

As a corollary, and in disagreement with previous work, it is found that in spite of the reorientation of $F_A(\text{Li}^+)$, the resonant Raman spectra originate mainly from the $F_A(\text{Li}^+)$ centers, which are properly oriented to absorb the exciting laser light.

ACKNOWLEDGMENTS

The authors would like to thank J. F. Zhou for his correspondence about some details of the behavior-type method for resonant Raman scattering and A. Bouwen for expert experimental assistance. Financial support from the Geconcerteerde Acties for W.J. and from the NFWO (Nationaal Fonds voor Wetenschappelijk Onderzoek) for M.L. is gratefully acknowledged. This work was performed under the auspices of, and supported by, the Geconcerteerde Acties and IIKW (Interuniversitair Instituut voor Kernwetenschappen) to which the authors are greatly indebted.

APPENDIX: NOTE ON THE EXTENSION OF THE BEHAVIOR-TYPE METHOD TO THE CASE OF RESONANT RAMAN SCATTERING

In order to facilitate the discussion on the extension of the BT method for RRS, some of the basic results of the BT method^{16,17} are reintroduced.

(i) The observed intensity I of a Raman mode of a particular point defect is a sum of intensities I_n , weighed by the population numbers $N^{(n)}$ of the defect in its n th possible orientation:

$$I = \sum_n N^{(n)} I_n . \quad (\text{A1})$$

(ii) For a particular optical geometry pair (OGP), determined by the pair of unit polarization vectors of the incident and the scattered field (\mathbf{a}, \mathbf{b}), the observed intensity I is written:

$$I = k I_0 \sum_{i,j,k,l=1}^3 a_i b_j a_k b_l P_{ijkl} , \quad (\text{A2})$$

in which the P_{ijkl} are the so-called intensity parameters (IP's), given by:

$$P_{ijkl} = \sum_{n=1}^{24} N^{(n)} T_{ij}^{(n)} T_{kl}^{(n)} . \quad (\text{A3})$$

$T^{(n)}$ is the Raman tensor of the defect in its n th orientation.

In general there are 81 IP's. For a real, symmetric tensor T , inspection of the number of independent products $T_{ij}^{(n)} T_{kl}^{(n)}$ shows that only 21 IP's are left. For an asymmetric tensor, i.e., in the case of RRS, this number increases to 45. It is obvious that only the IP's, which contain off-diagonal components of the Raman tensor, reflect the nonsymmetric form of the Raman tensor. As a result, the BT method for RRS, denoted by RRS BT, is necessary for the analysis of the polarized resonant Raman data of modes, which exhibit a nonzero depolarized scattering. On the other hand, the ordinary BT method still applies if only IP's of the form P_{ijij} and P_{iiii} contribute to the polarized Raman intensities. Examples of the latter situation are the modes of the $\text{Ti}^0(1)$ (Ref. 18) and Ti^+ -perturbed $\text{Ti}^0(1)$ center²³ under excitation in the third optical band, and the $F_A(\text{Li}^+)$ vibrations under F_{A1} excitation.

The RRS BT method is especially appropriate for the study of the low-frequency resonances of the $Tl^+Ti^{0(1)}$ center in KCl, RbCl, and KBr and for the 216-cm^{-1} mode of $F_A(Li^+)$ under F_{A2} excitation. We will not present an extensive discussion of the RRS BT method similar to the one in Ref. 16. Instead, a pragmatical extension has been performed, mainly focusing on the extended version of Tables VI, VII, and VIII of Ref. 16, which are the most essential ones for the interpretation of the experimental data. Reprints of these generalized tables are available upon request.

The RRS BT method is comparatively less powerful than the ordinary BT method, mainly because it deals with an enhanced number of IP's, necessitating the collecting of more polarized Raman data of sufficiently high accuracy. It is also less conclusive because of the following feature: Only 27 of the 45 IP's can be determined separately, while the other 18 IP's are obtained as terms in a sum of particular pairs of IP's. This is illustrated for the case of randomly oriented scatterers, where four independent IP's exist, namely:

$$P_{1111}, P_{1212}, P_{1122}, P_{1221}. \quad (A4)$$

Inspection of (A2) shows that the latter two IP's are measured together, since they always have the same proportionality factor $a_i b_j a_k b_l$. As a result, P_{1122} and P_{1221} cannot be determined separately and, moreover, the BT

relation r/q , which is very effective to identify "E-like" modes, cannot be verified anymore. Note that in the non-resonant case P_{1221} equals P_{1212} and the problem of separate determination does not occur.

Apart from the intrinsic drawbacks, it is useful to emphasize the experimental difficulties, caused by the resonant condition itself. First, the resonant enhancement of the light-scattering results in an extreme sensitivity of the polarized Raman intensities to the orientation of the sample, so that the determination of the observed BT may be obscured by misleading experimental IP values, due to relatively small orientation errors.¹⁸ Second, the incident polarized laser light may act as an effective orientating operator \hat{F} and this reduces the number of independent IP's, which can be determined. This problem was met in the study of $F_A(Li^+)$ in KCl and it is not superfluous to stress that it would be impossible to establish the A' character of the 216-cm^{-1} mode, based on the Raman data under F_{A2} excitation only. On the other hand, for all the defect systems that we have studied up until now with the resonant Raman technique, the dependence of the polarized Raman intensities on the excitation frequency, has shown to be helpful: some of the polarized Raman data, resulting from a particular excitation frequency can be analyzed by the simple BT method. If such a combined study with both the BT and the RRS BT method is possible, the analysis is much more conclusive.

¹F. Lüty, Z. Phys. **164**, 17 (1961).

²B. Fritz, F. Lüty, and G. Rausch, Phys. Status Solidi **11**, 635 (1965).

³R. L. Mieher, Phys. Rev. Lett. **8**, 362 (1962), and references therein.

⁴F. Lüty, in *Physics of Color Centers*, edited by W. B. Fowler (Academic, New York, 1968), p. 181.

⁵J. M. Worlock and S. S. Porto, Phys. Rev. Lett. **15**, 697 (1965).

⁶B. Fritz, in *Localized Excitations in Solids*, edited by R. F. Wallis (Plenum, New York, 1968), p. 496.

⁷F. Rosenberger and F. Lüty, Solid State Commun. **7**, 983 (1969).

⁸G. Baldacchini, G. P. Gallerano, U. M. Grassano, A. Lanciano, A. Sacco, F. Somma, M. Mencci, and M. Tonelli, Phys. Rev. B **33**, 4273 (1986).

⁹D. S. Pan and F. Lüty, in *Proceedings of the Third International Conference on Light Scattering in Solids, Campinas, Brazil, 1975*, edited by M. Balkanski, R. C. C. Leite, and S. P. S. Porto (Flammarion, Paris, 1975), p. 539.

¹⁰A. Mabud and F. Lüty, Abstract Book of the International Conference on Defects in Insulating Crystals, Salt Lake City, 1984 (unpublished), pp. 299 and 301.

¹¹V. Narayanamurti and R. O. Pohl, Rev. Mod. Phys. **42**, 201 (1970).

¹²D. Schoemaker and E. L. Yasaitis, Phys. Rev. B **5**, 4970

(1972).

¹³R. D. Kirby, A. E. Hughes, and A. J. Sievers, Phys. Rev. B **2**, 481 (1970).

¹⁴M. J. L. Sangster and A. M. Stoneham, Phys. Rev. B **26**, 1028 (1982).

¹⁵W. Joosen, E. Goovaerts, and D. Schoemaker, Phys. Rev. B **34**, 1273 (1986).

¹⁶J. F. Zhou, E. Goovaerts, and D. Schoemaker, Phys. Rev. B **29**, 5509 (1984).

¹⁷E. Goovaerts, J. F. Zhou, W. Joosen, and D. Schoemaker, Cryst. Lattice Defects Amorph. Mater., **12**, 317 (1985).

¹⁸W. Joosen, E. Goovaerts, and D. Schoemaker, Phys. Rev. B **32**, 6748 (1985); J. Lumin. **31-32**, 317 (1984).

¹⁹J. F. Zhou, E. Goovaerts, and D. Schoemaker, Phys. Rev. B **29**, 5533 (1984).

²⁰W. Joosen, J. F. Zhou, E. Goovaerts, and D. Schoemaker, Phys. Rev. B **31**, 6709 (1985).

²¹J. R. D. Copley, R. W. MacPherson, and T. Timusk, Phys. Rev. **182**, 965 (1969).

²²W. Joosen, M. Leblans, M. Vanhimbееck, H. De Raedt, E. Goovaerts, and D. Schoemaker, Proceedings of the Fifth European Topical Conference on Lattice Defects in Ionic Crystals, 1986 (unpublished). M. Vanhimbееck, H. De Raedt, W. Joosen, and D. Schoemaker (unpublished).

²³W. Joosen, E. Goovaerts, and D. Schoemaker (unpublished).